Journal of Instrumentation

A four-channels reflective Kirkpatrick-Baez microscope for the hot spot diagnostic in the 100 kJ laser driven inertial confinement fusion in China

To cite this article: X. Zhang *et al* 2019 *JINST* **14** C11010

Published by IOP Publishing for Sissa Medialab

Received: *June 30, 2019*
Revised: *September 8, 2019*
Accepted: *October 15, 2019*
Published: *November 11, 2019*

3rd European Conference on Plasma Diagnostics (ECPD2019)
6–10 May 2019
Lisbon, Portugal

A four-channels reflective Kirkpatrick-Baez microscope for the hot spot diagnostic in the 100 kJ laser driven inertial confinement fusion in China

X. Zhang,[a] Z. Chen,[a] Y. Li,[b] B. Mu,[a] W. Jiang,[a] J. Dong,[a] J. Yan,[a] B. Yu,[a] J. Xu,[b] X. Wang,[b] S. Liu,[a] Z. Yang,[a] L. Chen,[a] M. Chen,[a] Y. Dong,[a] Y. Pu,[a] T. Huang,[a] F. Wang,[a,1] S. Jiang,[a] J. Yang[a] and D. Yang[a]

[a] *Laser Fusion Research Center, China Academy of Engineering Physics, Mianshan Road No. 64, Mianyang, Sichuan, 621900, China*

[b] *School of Physics Science and Engineering, Tongji University, Siping Road No. 1239, Shanghai, 200092, China*

E-mail: lfrc_wangfeng@163.com

Abstract: A high quality hot spot is crucial in the laser driven inertial confinement fusion. The hot spot self-emitted X-ray images in a high spatial resolution may be used to analyze the hot spot asymmetry and some fine structures induced by mix. The high spatial resolved X-ray imaging diagnostics can also serve in the hydrodynamic instability growth radiography and some other physical research in the inertial confinement fusion. The Kirkpatrick-Baez microscope can provide a higher resolution and throughput efficiency diagnostic. A new four-channels KB microscope was designed and built for the < 10 keV X-ray imaging. The Pt coated reflective mirror pairs were used to obtain a wide grazing angle bandwidth. The variation of the X-ray reflectivity was small in a large field of view. The microscope had a magnification of about 20. The spatial resolution in the central field of view was about 7 µm. The similarities between the different channel images were about 97%. The KB microscope is in operation in the directly or indirectly driven implosions by 10–100 kJ lasers on Shenguang laser facility in China. The time-integral hot spot asymmetry has been diagnosed, and the time-resolved imaging will be implemented in the following work.

Keywords: Plasma diagnostics - interferometry, spectroscopy and imaging; Plasma diagnostics - high speed photography

[1]Corresponding author.

https://doi.org/10.1088/1748-0221/14/11/C11010

2019 JINST 14 C11010

Contents

1 Introduction

In the laser driven inertial confinement fusion (ICF), the capsule containing the fusion fuels implodes and forms a hot spot with a high temperature and a high density in a small size. The high quality hot spot is crucial to the ignition. In recent years, almost every laser driven ICF facility, including the National Ignition Facility (NIF) in US, is working on the improvement of the hot spot quality. The neutron yield on NIF has been increased so much, and the fusion energy output already exceeded the kinetic energy of the imploding shell [1–4]. However, the asymmetry and the mix of the hot spot are still the challenging problems in the path to ignition [5, 6]. The size of the hot spot is usually only several 10 µm. The self-emitted X-rays are continuum spectral, but the low energy X-rays will be self-absorbed much and the background will be high. So the high spatial resolution imaging diagnostics in a high X-ray energy band are necessary. Recently, the hydrodynamic instability growth radiography in the ICF [7, 8] and some other high energy density physics (HEDP) experiments also employ more and more high resolution imaging diagnostics.

The Kirkpatrick-Baez (KB) microscope is an advanced X-ray imaging system, with a high spatial resolution (several µm) and a high light collection efficiency ($\sim 10^{-7}$). It consists of two tandem orthogonally-placed mirrors with two grazing incidence angles [9]. The unique configuration makes the KB microscope be much easier to be assembled to a multi-channels imaging system than some other X-ray microscopes, like the bent crystal imager. And it is easy to be couple to a multi-chips time gated X-ray detector, to realize the time-resolved high resolution imaging. NIF has built some 4-channels KB microscopes [1, 11–13] for the hot spot diagnostics and the hydrodynamic instability growth radiography. A novel 16-channels KB microscope was designed and built on OMEGA [14–16], which was also already coupled to the time gated X-ray detector. There was a KB microscope designed and built on LMJ [17]. In the past years, there were also several KB microscopes with the multi-layer mirrors built on the Shenguang laser facility [18–21]. Some laser facilities for the HEDP experiment also developed some KB microscopes for the laser-plasma X-ray emission imaging [22]. Besides, some other X-ray microscopes based on the grazing incidence principle were designed and developed or under construction on the laser driven ICF facilities, like the toroidal mirrors microscope [23], the wolter-like microscope [24] and the wolter microscope [25–27]. The KB microscope can employ the full reflective mirrors and the multilayer coated mirrors. The full reflective mirrors have a higher energy-integral reflectivity and a wide grazing angle bandwidth, which means the reflectivity doesn't change too much when the grazing angle varies. It is possible to extend the effective field of view and mitigate the target pointing precision requirement. But it usually has a wide X-ray energy band. And the limit of X-rays energy is less than 10 keV. To achieve narrow band imaging and extend the X-ray energy to over 10 keV, the multilayer coated mirrors are the prior. But the grazing angle bandwidth limits the field of view and the requirement of pointing precision is higher. To balance the imaging X-ray energy limit and the grazing angle bandwidth, the non-periodic multilayer optics is proposed [28]. So the optics in the KB microscope can be chosen up to the image object feature and the X-ray energy.

In this work, a four-channels KB microscope was designed and built with the Pt coated reflective mirrors. The motivation of this microscope was the hot spot self-emitted X-ray imaging. And it was expected to be also appiled in the hydrodynamic instability growth radiography. Considering the present capsule areal density and the hot spot temperature, the X-ray energy bands of around 6 keV and 8 keV were fine in the hot spot imaging. The two energies could also be used in the Fe or Cu backlighter radiography. The design of the KB microscope was described in section 2, as well as the Ray-Trace simulations and the spatial resolution test. The time-integral hot spot imaging in the implosions were shown in section 3. The similarity of between the images of different channels was checked in section 3.1. The application of the KB microscope in the hot spot asymmetry diagnostics was described in section 3.2. Some conclusions were followed in section 4.

2 The KB microscope with reflective mirrors

A new KB microscope was assembled in Tongji University and applied in the laser driven ICF experiments in Laser Fusion Research Center in China. To decrease the reflectivity variation in a relatively wide field of view, the KB microscope was designed with the reflective mirrors and a small grazing angle. The configuration of the KB microscope is shown in figure 1(a). The principle of "mirror sharing" was adopted in the design. The microscope objective consisted of two pairs of the super-polished concave spherical mirrors, to form four symmetrical imaging channels. Each mirror contributed in two channels. There were four small apertures in front of the four corners of the orthogonally-placed mirrors, as shown in figure 1(b). The focus equation of each mirror in one channel can be described by

$$\frac{1}{u} + \frac{1}{v} = \frac{2}{R\sin\theta_1} \tag{2.1}$$

$$\frac{1}{u+d} + \frac{1}{v-d} = \frac{2}{R\sin\theta_2}, \tag{2.2}$$

where u and v were the object distance and image distance of the first mirror respectively, R was the curvature radius of the mirrors, d was the length of the mirror, θ_1 and θ_2 were the grazing angles of the first and second mirror respectively. The optics design was summarized in table 1. The image recorder could be an imaging plate for the static imaging or a time gated X-ray detector for the time-resolved imaging. The four images were arranged at the four corner of a square, with a distance of 20 mm.

2019 JINST 14 C11010

Table 1. Optic Design of the KB microscope.

Mirror	Curvature Radius	Length (d)	Object Distance	Image Distance	Central Grazing Angle	Magnification
Meridian Mirror	50 m	12 mm	200 mm	4200 mm	0.4375°	21
Sagittal Mirror	50 m	12 mm	212 mm	4188 mm	0.4625°	19.8

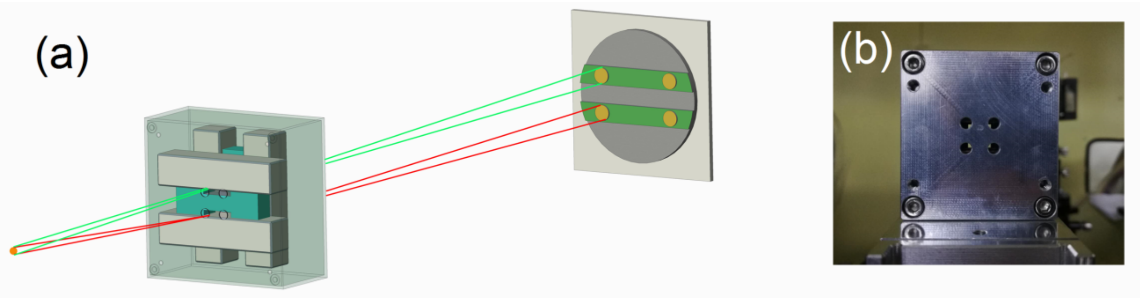

Figure 1. Schematic(a) of the four-Channels Reflective KB microscopes and the photos in a front view(b).

The mirrors were super-polished spherical Si substrates, coated with a Pt film of several nm in thickness. The roughness of the mirror surface was less than 0.3 nm. The curvature radius deviations of the four spherical mirrors were about 3 ~ 8%. A steel frame and two H-shaped cores in a high precision of fabrication were utilized to position the two layers of the mirror pairs. During the alignment, each mirror could be adjusted in a very small range to mitigate the astigmatism from the curvature radius deviation. This microscope was proposed to image the X-rays around 6 keV or 8 keV from the hot spot or the laser driven backlighters, like Cu or Fe. The incidence grazing angles were far away from the Pt full reflectivity edge to 8 keV X-rays, to obtain a wider grazing angle bandwidth. As a result, the microscope could get a relatively flat reflectivity in a wide field of view, and the tolerance of the pointing of the sightline could be improved. The reflectivity of the Pt mirror pair to the energy of the X-rays with the central grazing angles was calculated and shown in figure 2. Usually there were 50 µm Be and 25 µm Al filters in the X-ray path, to eliminate the lower energy X-rays and shield the target debris. In addition, 20 µm Fe filter or 20 µm Ni filter could be added into the X-ray path, to narrow the X-ray energy band by the K-edge. The X-ray reflectivity of the mirror pair in a wide field of view was calculated by a Ray-Trace code. The calculated reflectivity maps of 6 keV and 8 keV X-rays are shown in figure 3. To the 6 keV X-rays, the variation of reflectivity is less than ±0.1 in a range of ±200 µm. And to the 8 keV X-rays, it is about ±0.15 in the central field of 400µm. It means that if the object is large in the field of view, or if there is a 100 µm pointing deviation, the image will not deform too much. At present, the reflectivity map of each channel is not able to be measured directly. An X-ray optic calibration facility is in plan, in which the X-ray source will be designed with two switchable X-ray tubes. One of them will be a tube with a spot size of ~ 2 mm, and the other one will be a micro-focus x-ray tube with a spot size of 10–20 µm.

This KB microscope was already installed on the Shenguang Laser Facility. It was first used to image a metal grid with a laser driven X-ray backlighter. The grid had 1500 periods per inch, which had a periodicity of 16.9 µm and bars of 6 µm. The backlighter was Cu driven by 4 laser beams

2019 JINST 14 C11010

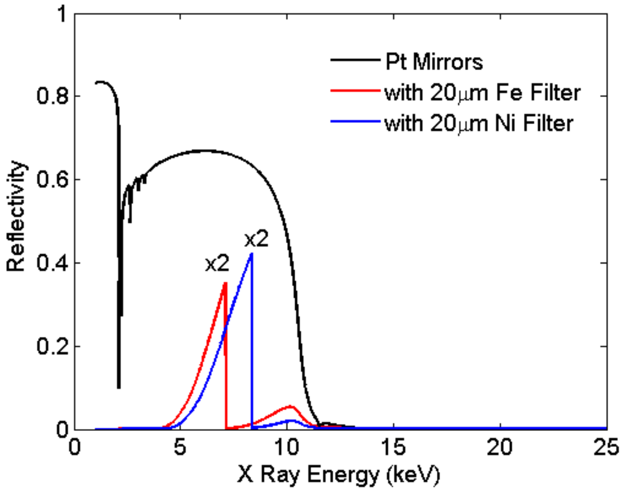

Figure 2. The calculated reflectivity of the mirror pair (Black line) and the calculated throughput efficiency with 50 μm Be, 25 μm Al, 20 μm Fe or Ni filters (Red and Blue lines, with double values).

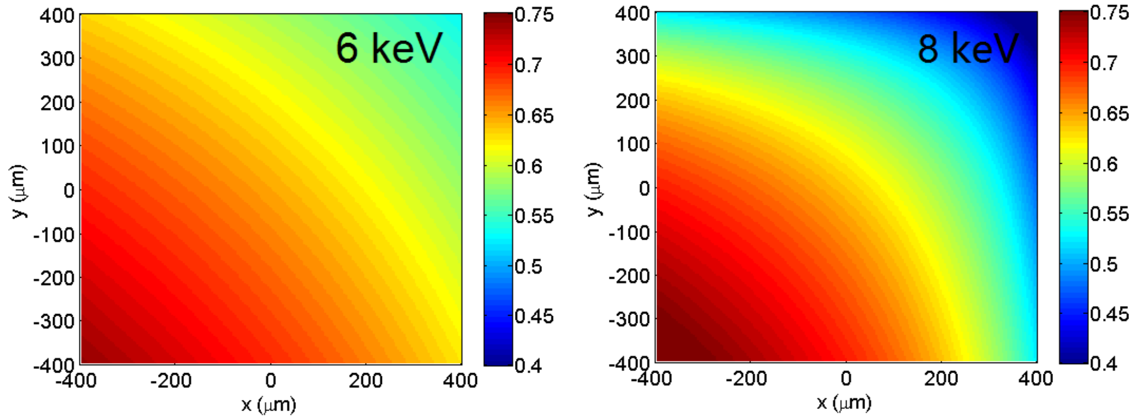

Figure 3. The Ray-Trace code calculated reflectivity maps of the mirror pair to the 6 keV and 8 keV X-rays.

with a total energy of about 3 kJ in 1ns. The diameter of the laser spot was about 500 μm. The images were recorded with an imaging plate, type of Fuji SR2025. The image in the first channel is shown in figure 4(a). Due to the non-uniform illumination, the intensity is high in the center, and it falls down along the X direction and the Y direction. The cross sections in the X and Y directions are shown in figure 4(b) and 4(c) respectively. According to the edges of the cross sections at the positions close to $X = 0$ and $Y = 0$, the spatial resolution was estimated to be about 7 μm in the central region of the field of view. The spatial resolution deteriorates when the viewing position moves away from the center. The behaviors of the backlighting grid images in the other 3 channels are similar.

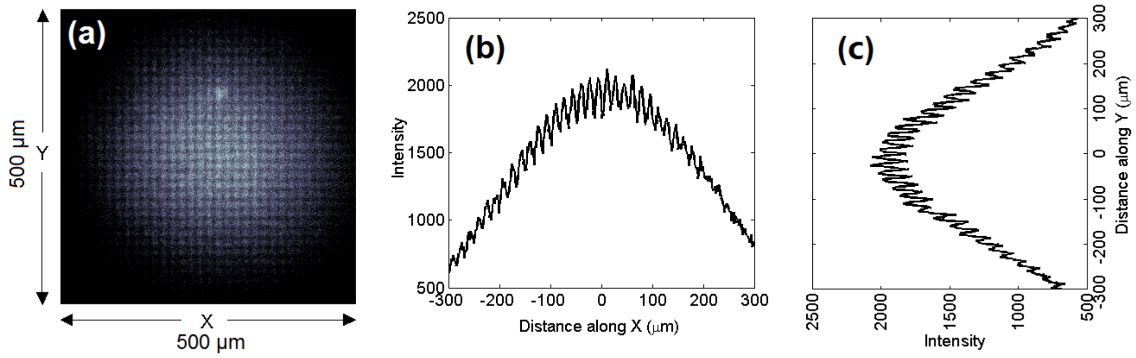

Figure 4. The grid image (a) by a Cu backlighter and the cross sections along X axis (b) and Y axis (c).

3 The measured time-integral images of the hot spot in the implosions

The KB microscope in this work was proposed to diagnose the hot spot image in the laser driven ICF, and could also be applied in the X-ray backlighted Hydro-dynamic instability growth radiography. The time-resolved imaging can be implemented by the combination of the KB microscope and a time gated X-ray detector. However, before the time resolved imaging diagnostics in operation, it was necessary to guarantee the static images of different imaging channels were the same. In this work, the similarities of the images in the four channels of the KB microscope were checked by the time-integral images measurement of the hot spot in an exploding target. And then it was used to measure the time-integral hot spot images in the laser indirectly driven implosion experiment.

3.1 Similarity check of the images in different imaging channels

The KB microscope firstly operated in the laser directly driven exploding target experiments. The exploding target consisted of only a glass capsule, without the holhraum or any other covers. It was easily to be pointed in a high precision, and the difference among the different channel images due to the mis-pointing could be suppressed. The target pointing scheme of this KB microscope was the same as that in reference [20]. A mechanical module of the optical binocular system was assembled. The exploding target had a small convergence ratio. It usually presented a large hot spot and a high temperature. It could contribute a large X-ray source in size with a high intensity, which benifited the similarity check in a large spatial range.

In this work, the exploding target consisted of a capsule with 540 μm in diameter. The shell was SiO_2 and 2 μm in thickness. It was filled in 10atm D_2 gas. The targets in this work were fabricated by the target fabrication team in Laser Fusion Research Center [29, 30]. The exploding target was irradiated by 48 laser beams with a total energy of about 40 kJ in 1ns. The filters in the KB microscope were 20μm Fe, 50 μm Be and 25 μm Al. The time-integral images of the four channels were recorded by an Imaging Plate, as shown in figure 5. The size and the structure of hot spot images looks the same, as well as the halo generated during the glass shell ablation and the support bar in the right side. The similarity [31, 32], r, between two images is defined as equation (3.1), where $\overline{A}$ and $\overline{B}$ are the mean intensity in a specified range of the two images, A_{mn} and B_{mn} are the intensities of each pixel. In figure 5, the similarities under the 30% contours between the 1st channel image and the 2nd, 3rd and 4th channel images are 99.3%, 98.3% and 97.8%, respectively.

The similarities under the 50% contours and 80% contours are aslo over 96%. The small differences may be resulted from the different background noise levels and the small assembling deviations between the assembled mirrors and the design. To reduce the noise, the design of the imaging path will be optimzed in the next KB microscope. It is suggested to adopt a crossing aperture in the imaging path as that in reference [11, 12] and enclose the mirrors module and the imaging module in a sealed tube. The calibration of the reflectivity and spatial resolution will be also implemented.

$$r = \frac{\sum_m \sum_n \left(A_{mn} - \overline{A}\right)\left(B_{mn} - \overline{B}\right)}{\sqrt{\left(\sum_m \sum_n \left(A_{mn} - \overline{A}\right)^2\right)\left(\sum_m \sum_n \left(B_{mn} - \overline{B}\right)^2\right)}} \tag{3.1}$$

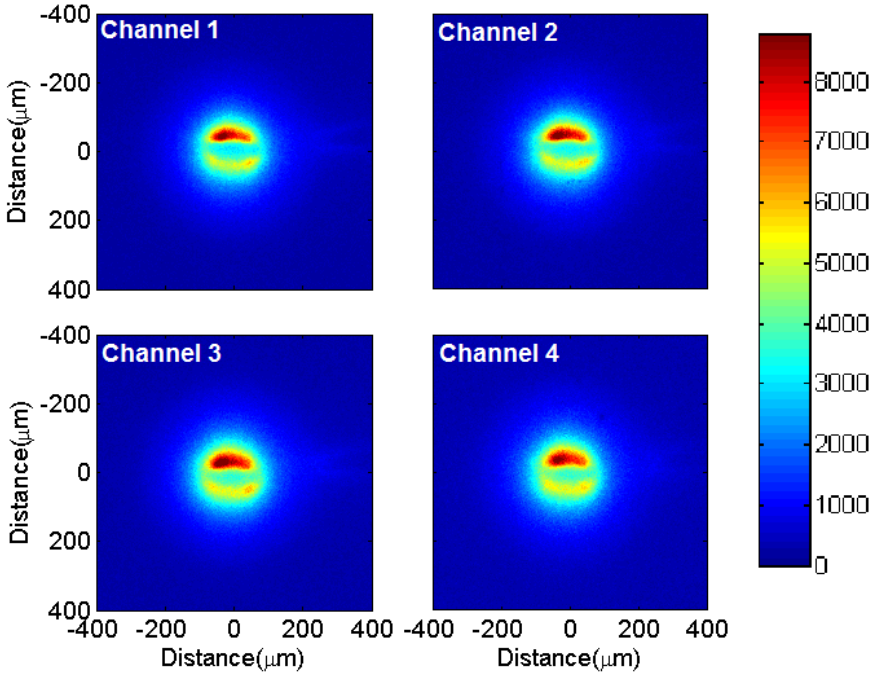

Figure 5. The recorded time-integral images of an exploding target in the four channels of the KB microscope.

3.2 Hot spot imaging in the laser indirectly driven implosion

The KB microscope was already involved in the hot spot imaging diagnostics for the laser indirectly driven implosion on Shenguang laser facility. It was able to provide the hot spot images with a higher spatial resolution than the pinhole imaging in the 100 kJ laser driven implosions. Furthermore, it could diagnose the hot spot asymmetry and the fine structures in the hot spots. After the intensity and energy response calibration of the microscope and the recorder, it may be also used to study the mix in the hot spot. Some calibration methods are proposed [13, 33, 34]. The KB microscope was installed on a general diagnostics instrument manipulator (DIM) and inserted inside the vacuum chamber. It can be installed with an equatorial view or a polar view. This KB microscope was supposed to image the hot spot when the areal density was not too high. So the mesured X-ray

2019 JINST 14 C11010

energy would not be higher than 10 keV. The energy band could be set in 5.7–7.1 keV be the Fe filter and 6.5–8.3 keV by the Ni filter, as shown in figure 2. For the shots with a low X-ray emission, only Be and Al filters would be utilized, and the energy band would be a little wider.

At present, the KB microscope was operated in the time-integral imaging mode. The images were recorded by an Imaging Plate. Figure 6 shows a measured hot spot image in a gas filled cylindrical hohlraum driven implosion. The microscope used the Fe filter in this shot, and it was installed in the equatorial view. The microscope collected the hot spot X-rays through a 300 µm × 300 µm diagnostic aperture on the waist of the hohlraum. The capsule had a 65 µm CH shell and an inner diameter of 750 µm, filled in 10atm D_2 gas. With a total laser energy of 80 kJ, the capsule was driven by a two-step radiation pulse (figure 6(a)). The hot spot presented a "pancake" shape, and the neutron yield over clean calculation (YOC) was as low as 10%. The green line in figure 6(b) was the 50% contour of the hot spot image. By fitting with the Legendre polynomial, it was found that the P2 fraction was about −0.26 and the P4 fraction was about 0.03. In this shot, a static pinhole X-ray imager in a polar view monitored the laser spots postion through the laser entrance hole. The angle between the its sightline and the cylindrical axis was 16 degree. It found that the laser spots moved inside about 200 µm to the cylindrical axis. As a result, the X-ray radiation on the capsule had a stronger polar driven, and hot spot presented a "pancake" asymmetry as that in figure 6(b). The anomalous laser spot movement might be due to the leak of the hohlraum gas, which would make the wall plasmas moved faster toward to the cylindrical axis.

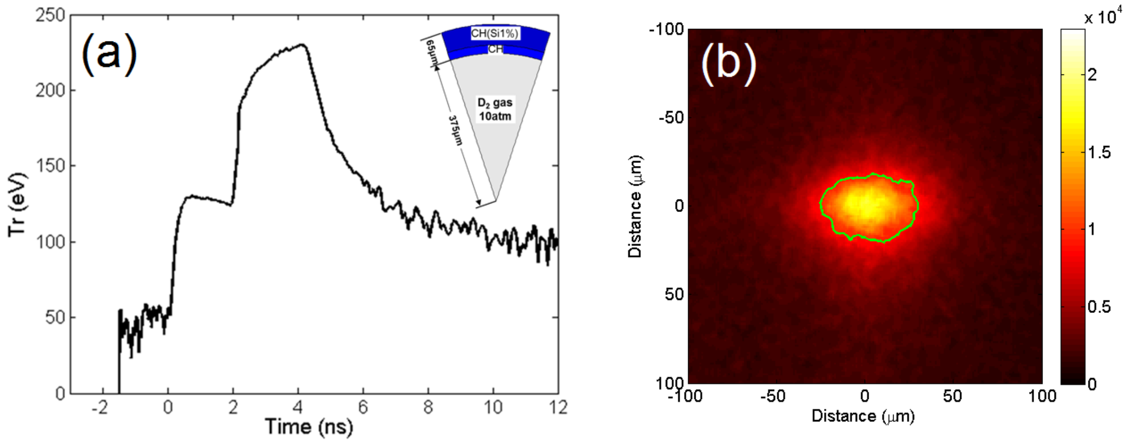

Figure 6. The measured hot spot image (b) of a two-step radiation pulse (a) driven capsule (insert figure in a).

4 Conclusions

A new four-channels KB microscope was built and in operation on Shenguang laser facility in China. The microscope was designed with the Pt coated reflective mirror pairs, to obtain a wide grazing angle bandwidth. As a result, the variation of the X-ray reflectivity was small in a large field of view. It could also be applied in the radiography of an object with a relatively large size. The microscope had a large magnification and a spatial resolution about 7 µm in the central field of view. It was able to diagnose the hot spot asymmetry in the laser driven ICF. The similarities between the

2019 JINST 14 C11010

images of different channels were about 97%. The KB microscope has been used to diagnose the implosion hot spot in the laser indirect driven ICF. At present, only time-integral hot spot images were measured. The asymmetry of the hot spot was obtained and consistent with the estimation. In the following work, the KB microscope will be couple to a time gated X-ray detector. The time gated X-ray detector is in an air box. Both of the KB microscope and the time gated X-ray detector will be installed in the same DIM. The calibrations of the reflectivity and energy responses of the microscope and the recorder are also in plan. In future, the next KB microscope on our facility will be designed with an optimized structure to reduce the background noise and improve the pointing precision. The KB microscopes with multi-periodic layer mirrors and non-periodic layer mirrors will also be considered to extend the imaging X-ray energy to be above 10 keV.

Acknowledgments

This work was supported by the National Key R&D Program of China (2017YFA0403200) and the National Natural Science Foundation of China under Grants (Nos. 11705178, 11605178, and 11805178). The authors are very grateful to the Laser Facility Operation Team and the Target Fabrication Team in Laser Fusion Research Center.

References

[1] O.A. Hurricane, P.T. Springer, P.K. Patel, D.A. Callahan, K. Baker, D.T. Casey et al., *Approaching a burning plasma on the NIF*, *Phys. Plasmas* **26** (2019) 052704.

[2] S. Le Pape, L.B. Hopkins, L. Divol, A. Pak, E. Dewald, S. Bhandarkar et al., *Fusion energy output greater than the kinetic energy of an imploding shell at the national ignition facility*, *Phys. Rev. Lett.* **120** (2018) 245003.

[3] O.A. Hurricane, D.A. Callahan, D.T. Casey, E.L. Dewald, T.R. Dittrich, T. Döppner et al., *Inertially confined fusion plasmas dominated by alpha-particle self-heating*, *Nat. Phys.* **12** (2016) 800.

[4] O.A. Hurricane, D.A. Callahan, D.T. Casey, P.M. Celliers, C. Cerjan, E.L. Dewald et al., *Fuel gain exceeding unity in an inertially confined fusion implosion*, *Nature* **506** (2014) 343.

[5] Y. Li, C. Zhai, G. Ren, J. Gu, W. Huo, X. Meng et al., *P2 asymmetry of au's m-band flux and its smoothing effect due to high-z ablator dopants*, *Matter Radiat. Extrem.* **2** (2017) 69.

[6] J. Gu, Z. Dai, S. Zou, W. Ye, W. Zheng, P. Gu et al., *Effects of mode coupling between low-mode radiation flux asymmetry and intermediate-mode ablator roughness on ignition capsule implosions*, *Matter Radiat. Extrem.* **2** (2017) 9.

[7] L.A. Pickworth, B.A. Hammel, V.A. Smalyuk, H.F. Robey, R. Tommasini, L.R. Benedetti et al., *Development of new platforms for hydrodynamic instability and asymmetry measurements in deceleration phase of indirectly driven implosions on NIF*, *Phys. Plasmas* **25** (2018) 082705.

[8] L.A. Pickworth, B.A. Hammel, V.A. Smalyuk, H.F. Robey, L.R. Benedetti, L.B. Hopkins et al., *Visualizing deceleration-phase instabilities in inertial confinement fusion implosions using an "enhanced self-emission" technique at the national ignition facility*, *Phy. Plasmas* **25** (2018) 054502.

[9] P. Kirkpatrick and A.V. Baez, *Formation of optical images by x-rays*, *J. Opt. Soc. Am.* **38** (1948) 766.

[10] L.A. Pickworth, T. McCarville, T. Decker, T. Pardini, J. Ayers, P. Bell et al., *A kirkpatrick-baez microscope for the national ignition facility*, *Rev. Sci. Instrum.* **85** (2014) 11D611.

2019 JINST 14 C11010

[11] L.A. Pickworth, J. Ayers, P. Bell, N.F. Brejnholt, J.G. Buscho, D. Bradley et al., *The national ignition facility modular kirkpatrick-baez microscope*, *Rev. Sci. Instrum.* **87** (2016) 11E316.

[12] M.J. Ayers et al., *Engineering Precision Relocation Capability into a Large-Cantilevered telescoping Diagnostic for a Kirkpatrick-Baez X-ray Optic*, *Proc. SPIE* **9211** (2014) 92110C.

[13] N.F. Brejnholt et al., *Calibration results for first NIF Kirkpatrick-Baez microscope*, *Proc. SPIE* **9591** (2015) 95910J.

[14] F.J. Marshall, *Compact kirkpatrick–baez microscope mirrors for imaging laser-plasma x-ray emission*, *Rev. Sci. Instrum.* **83** (2012) 10E518.

[15] F.J. Marshall, R.E. Bahr, V.N. Goncharov, V.Y. Glebov, B. Peng, S.P. Regan et al., *A framed, 16-image kirkpatrick–baez x-ray microscope*, *Rev. Sci. Instrum.* **88** (2017) 093702.

[16] F.J. Marshall, J.A. Oertel and P.J. Walsh, *Framed, 16-image, kirkpatrick–baez microscope for laser–plasma x-ray emission*, *Rev. Sci. Instrum.* **75** (2004) 4045.

[17] R. Rosch, J.Y. Boutin, J.P. le Breton, D. Gontier, J.P. Jadaud, C. Reverdin et al., *X-ray imaging with grazing-incidence microscopes developed for the LIL program*, *Rev. Sci. Instrum.* **78** (2007) 033704.

[18] B.Z. Mu et al., *Design and fabrication of X-ray Kirkpatrick-Baez microscope for ICF*, *Proc. SPIE* **6722** (2007) 67220S.

[19] Y. Li, B. Mu, Q. Xie, Y. He, Z. Chen, Z. Wang et al., *Development of an x-ray eight-image kirkpatrick–baez diagnostic system for china's laser fusion facility*, *Appl. Opt.* **56** (2017) 3311.

[20] Y. Li, J. Dong, Q. Xie, J. Xu, H. Liu, W. Li et al., *Development of a polar-view kirkpatrick-baez x-ray microscope for implosion asymmetry studies*, *Opt. Express* **27** (2019) 8348.

[21] Q. Xie, B. Mu, Y. Li, X. Wang, Q. Huang, Z. Wang et al., *Development of high resolution dual-energy KBA microscope with large field of view for RT-instability diagnostics at SG-III facility*, *Opt. Express* **25** (2017) 2608.

[22] D.A. Vikhlyaev, D.S. Gavrilov, A.G. Kakshin, A.V. Potapov and K.V. Safronov, *Four-channel x-ray microscope for plasma investigations on the sokol-p laser facility*, *Quantum Electron.* **41** (2011) 234.

[23] R. Rosch, C. Trosseille, T. Caillaud, V. Allouche, J.L. Bourgade, M. Briat et al., *First set of gated x-ray imaging diagnostics for the laser megajoule facility*, *Rev. Sci. Instrum.* **87** (2016) 033706.

[24] P. Troussel, B. Meyer, R. Reverdin, B. Angelier, G. Lidove, P. Salvatore et al., *Wolter-like high resolution x-ray imaging microscope for rayleigh taylor instabilities studies*, *Rev. Sci. Instrum.* **76** (2005) 063707.

[25] J.K. Vogel, M.J. Pivovaroff, B. Kozioziemski, C.C. Walton, J. Ayers, P. Bell et al., *Design and raytrace simulations of a multilayer-coated wolter x-ray optic for the z machine at sandia national laboratories*, *Rev. Sci. Instrum.* **89** (2018) 10G113.

[26] J.R. Fein, D.J. Ampleford, J.K. Vogel, B. Kozioziemski, C.C. Walton, M. Wu et al., *A wolter imager on the z machine to diagnose warm x-ray sources*, *Rev. Sci. Instrum.* **89** (2018) 10G115.

[27] M. Wu, B. Kozioziemski, J.K. Vogel, P. Lake, J.R. Fein, D.J. Ampleford et al., *Characterization and calibration of a multilayer coated wolter optic for an imager on the z-machine at sandia national laboratories*, *Rev. Sci. Instrum.* **89** (2018) 10G114.

[28] P. Troussel, D. Dennetiere, A. Rousseau, S. Darbon, P. Høghøj, S. Hedacq et al., *Applications of non-periodic multilayer optics for high-resolution x-ray microscopes below 30 keV*, *Rev. Sci. Instrum.* **83** (2012) 10E533.

[29] K. Du, M. Liu, T. Wang, X. He, Z. Wang and J. Zhang, *Recent progress in ICF target fabrication at RCLF*, *Matter Radiat. Extrem.* **3** (2018) 135.

[30] M. Liu, Y. Huang, S. Chen, D. Pan, M. Chen, Q. Chu et al., *Progress and challenges in the fabrication of DPS shells for ICF*, *Matter Radiat. Extrem.* **4** (2019) 018401.

[31] W.H. Press et al., *Numerical Recipes in Fortran: The Art of Scientific Computing*, 2nd edition, Cambridge University Press, Cambridge (1992).

[32] L. Gonick and W. Smith, *The Cartoon Guide to Statistics*, Harper Perennial, New York (1993).

[33] Y. Li, Q. Xie, Z. Chen, Q. Xin, X. Wang, B. Mu et al., *Direct intensity calibration of x-ray grazing-incidence microscopes with home-lab source*, *Rev. Sci. Instrum.* **89** (2018) 013704.

[34] B.J. Kozioziemski, J. Ayers, P. Bell, D.K. Bradley, M.-A. Descalle, S. Hau-Riege et al., *An x-ray optic calibration facility for high energy density diagnostics*, *Rev. Sci. Instrum.* **89** (2018) 10G112.

2019 JINST 14 C11010